February 2014

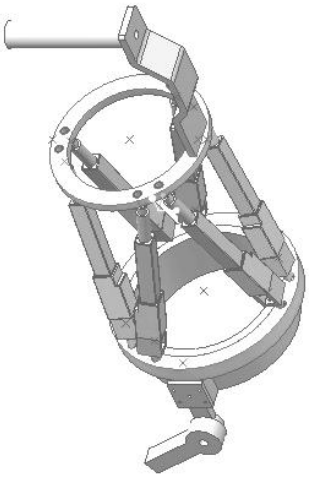

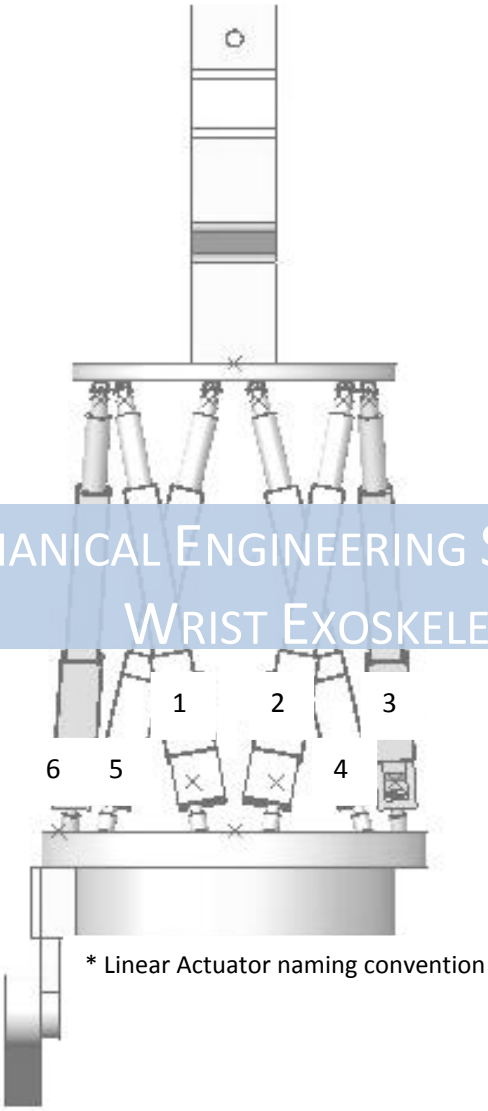

* Linear Actuator naming convention

IN LUMINE TUO

MECHANICAL ENGINEERING SENIOR DESIGN: WRIST EXOSKELETON

Mechanical Engineering Department
Columbia University
In Lumine Tuo Videbimus Lumen

Wrist Exoskeleton, In Lumine Tuo
MECE3430 Senior Design, Professor Stolfi
ME Department Columbia University 2014

Authors: Yoo Chan Chang, Zaoyuan Ge, Samuel Guo, Kyle Hom, Nathan Rodriguez

February 2014

Executive Summary:

The main objective of this Senior Design Project is to develop a functioning Stewart Platform prototype as a model of the human wrist. A Stewart Platform is a parallel plane mechanism that incorporates six actuators, providing six degrees of freedom. For our purposes developing the motion of the wrist requires only 2 degrees of freedom (the pitch and yaw rotational DOF). In order to achieve the wrist motion, 4 DOF will have to be constrained—the x, y, and z translational DOF and the rotational roll to be exact. By constraining the DOFs using the control system, we constrain the 6 DOF mechanism to 2 degree functionality.

The vision for our Stewart Platform (SP) is to provide a exoskeleton design for the arm to fit—encapsulated by the SP. Inspired by the Raytheon Sarcos[1] full-body exoskeleton, our wrist exoskeleton can have a wide range of application fields. However, for our purposes we choose to select the rehabilitation of stroke patients requiring neurorehabilitation.[2] A known treatment of stroke related impairments has been movement therapy. Studies have shown that limb stimulation can lead to synaptogenesis and the re-establishment of the neural pathways that control volitional movement, potentially leading to impairment reduction, added functional capabilities, and reduced disabilities.[3] As a future application, our SP can be used for muscle degenerative diseases (future application), specifically neuromuscular diseases like Inclusion Body Myositis.[4] This disease is characterized by slowly progressive weakness in wrist flexor muscles. Therefore, our application is to provide rehabilitation through mobility-gait training with an assistive device.

Introduction:

Upon our initial literature search, SPs have a wide set of applications varying from aerospace simulation training to LIDS (Low Impact Docking Systems) employed by NASA to manipulate space vehicles. However, the mathematics behind the SP allows for large to small size applications. The SP consists of 2 rigid frames connected by 6 variable length legs.

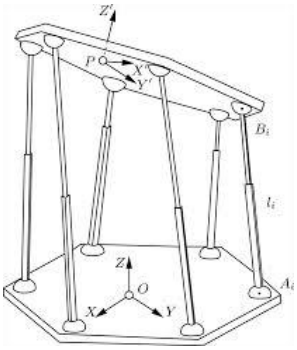

For our purposes, the base frame is considered to be the reference frame work. The mechanism has 6 degrees of freedom with respect to the base; 3 translational displacements and 3 angular displacements. Since the motion of the

[1] Raytheon Corporation Product, Military Application http://www.raytheon.com/newsroom/technology_today/2009_i1/feature_10.html

[3] Robot-Aided Neurorehabilitation: A Robot for Wrist Rehabilitation; http://www.ncbi.nlm.nih.gov/pmc/articles/PMC2733849/

[4] Novel therapeutic approaches for inclusion body myositis; http://www.myositis.org/storage/documents/General_Research/IBM_Published_Research/Novel_therapeutic_approaches.pdf

SP can be defined by rotational matrices, the properties of the SP are independent of the size and therefore can be applied to mimic the human wrist. In addition, the forward and inverse kinematic analysis of our 6 linear actuator device will be discussed later in this paper. The procedure chosen in providing our final analysis is given an in depth discussion. Although the SP is a common mechanism used in aerospace application, our literature research revealed that its application focused upon a wrist exoskeleton is a novel approach for the usage of the SP.

In this report, the specifications and parameter analysis for the dimensions and materials of the SP are examined. Through the usage of Creo's force and position analysis we were able to obtain data supporting our engineering design concepts. The calculations discussed later in the paper provide adequate information for deciding our engineering design. In addition, the final design describes the layout of our SP with drawings and sketches of the operation of our device.

Finally, the plan for the manufacturing process, problem analysis of the risks involved with our design, and the machining description of each part is covered in this report.

Literature Review

The inspiration for our hand-to-wrist exoskeleton partially originated from the Titan Arm[5], the winner of the 2013 Cornell Cup. We were intrigued by its simplicity and functionality and wanted to improve upon the project, eventually coming to the idea for a motorized wrist movement. The proposed design of the hand-to-wrist exoskeleton is a parallel-actuated platform, which angles a plane about a point, fitted around the wrist via a clamp system. Alternative actuation approaches include creating a series-actuated joint with motors or a hydraulically driven platform. While pneumatics/hydraulics are highly desirable for their power- for their power-to-mass and power-to-volume ratios, these actuators are too expensive and bulky for our design. From the literature researched, the parallel-actuated systems offered the best size and performance characteristics.

A key discovery in our research was the Stewart Platform, which is the main component of our motorized wrist design. The Stewart Platform is driven by 6 (typically hydraulic) actuators connected in series connecting two initially parallel platforms. The most appealing aspects of the Stewart Platform are the six DOF in a closed-chain fashion and a compact envelope. These characteristics especially suit the Stewart Platform's compatibility with the wrist's modeling as a ball-and-socket joint. As constructed in the Rice Wrist by Rice University's Gupta, O'Malley, Patoglu, and Burgar, modeled by Agrawal, Desmier, and Li[6], and analyzed in a Stewart Platform Wrist by Nguyen et. al[7] in NASA's Goddard Space Center, the motions generated by the Stewart Platform strongly mirror the wrist's, suggesting that it can be used as a mechanical wrist joint.

A patent by Aguirre-Ollinger et. al[8] focuses on the control system, another aspect to

[5] Retrieved from http://titanarm.com/.

[6] Agrawal, S. K., Glen Desmier, and Siyan Li. "Fabrication and Analysis of a Novel 3 DOF Parallel Wrist Mechanism." *Journal of Mechanical Design, Transactions Of the ASME* 117.2 A (1995): 343-5. *SCOPUS.*Web. 15 Oct. 2013.

[7] Nguyen, C. C., et al. "Analysis and Implementation of a 6 DOF Stewart Platform-Based Robotic Wrist." *Computers and Electrical Engineering* 17.3 (1991): 191-203. *SCOPUS.* Web. 15 Oct. 2013.

[8] Aguirre-Ollinger, Gabriel, Ambarish Goswami, J. Edward Colgate, and Michael A. Peshkin. Controller For An Assistive Exoskeleton Based on Active Impedance. Honda Motor Co., Ltd.; Northwestern

consider in the design of the exoskeleton. Instead of having the user be the one to execute all the movements, a controller is implemented. The primary role of this controller is to amplify the user's forces from the arm via EMG signals. The exoskeleton itself will prove that it is capable by displaying active impendence. The patent also shows multiple diagrams of not only the transfer functions with its components but incorporates actual human motion that can be modeled within the transfer function. By studying these transfer functions and diagrams, we can adapt the functions to be modeled after the wrist with two DOFs.

Concept Generation/Concept Selection:

A major discussion over the design of the SP was focused on the type of actuation. During our first iteration of the design we rested on 3 choices for the actuators. The first choice for the actuators was a hydraulic piston cylinder, followed by the use of linear actuators or pneumatic piston cylinders. Each actuator provides its own benefits to the exoskeleton system. Hydraulics presents the most strength output in comparison to the other actuators and therefore for any strength application, this system would be most desirable. In addition, hydraulic pistons require a pump, specialized control system and a reservoir to store the fluid. Linear actuators provide an actuation system with high accuracy and relatively strong power output. As a result, linear actuators would be the most desirable actuator for any application requiring accuracy. Finally, pneumatic pistons provide the cheapest option per actuator for motion while adding amplified strength and speed of motion. However, for pneumatic pistons additional pumps, valves, and an air tank reservoir are required for its operation.

Therefore, inspiration for our selection of actuator systems largely stemmed from our application selection. Since we desired to have a rehabilitative device for the gait-training of the wrist's motion, the most desirable choice for the SP motion generation was linear actuators. In addition to featuring position control as part of the mechanism, the linear actuators can be easily powered by a control board.

Aside from the actuation system of the SP, significant investigation was performed for the material composition of the exoskeleton. Some major points of focus were on the product's weight, durability, and ease of manufacturing processes. Materials such as aluminum and steel provide great strength capabilities but greatly influence the overall weight of the device. Therefore, after further investigation into material properties we decided on the use of delrin as the base and top parallel planes. Delrin (Acetal Homopolymer) is a crystalline plastic which offers an excellent balance of properties that bridge the gap between metals and plastics. This material possesses high tensile strength, stiffness and toughness, a great strength-to-weight ratio, and exhibits excellent machinability properties. In addition, acetal plastic is employed in the universal joints of the SP because of its high strength, stiffness, and good wear resistant properties. For the elbow joint and connector pieces, aluminum was selected because of the required durability and safety factor for our device.

Final Concept Description:

The final concept description consists of 3 components: the elbow joint/connections, the SP, and the control system design. The elbow

University, assignee. Patent US 7,731,670 B2. 8 June 2010. Print.

joint will be machined using two concentric cylinders with a bushing between to allow rotation. For the attachment of the elbow joint to the bicep mold a simple procedure of a strap/screw system will hold it in place. For easy attachment to the hand of the patient, our design incorporates a rod attachment located at the top of the SP that allows the patient to grip the device. Given that the state of the patient may inhibit the gripping action, the rod will have a strap that will securely attach to the patients hand. Therefore, the motion of the SP will be transferred to the patient's risk via the rod attachment. The SP design has already been heavily described, but the importance of the SP to the exoskeleton permits re-summarizing the design. SPs are parallel plane mechanisms that enable 6 DOFs through the motion of 6 independent actuators. By constraining 4 DOFs of the top disc, namely the x, y, and z translational degrees and the roll rotational degree of freedom, we will enable the SP to provide the necessary workspace for the motion of the human wrist.

For the control system, our primary concern is the actuator lengths. The control system will be composed of two feedback loops. The first loop will be used to command the actuator to achieve the desired lengths, as determined by our inverse kinematics, and correct any deviations or error in our signal. The second loop is embedded in the linear actuator for position feedback control that will allow us to decrease the actuator length error to zero. The selected linear actuators feature integrated controllers for position and speed control, which simply requires RC or PWM commands to be sent from a control board. Because of the wide variety of poses desired, a large onboard memory is required.

Specifications and Parameter Analysis: Inverse Kinematic Analysis

Our SP rotates and is capable of translation by the extension and contraction of its linear actuators. Therefore, length of each linear actuator will be the output of our control system. Kinematic analysis is crucial to controlling our exoskeleton to achieve desired motion/configuration precisely. The objective of our kinematic analysis is to know the exact length of each linear actuator at any desired configuration. The core idea behind our inverse kinematics can be summarized in two steps: expressing the coordinates of actuator's two ends in one coordinate system and then finding the length between the two ends.

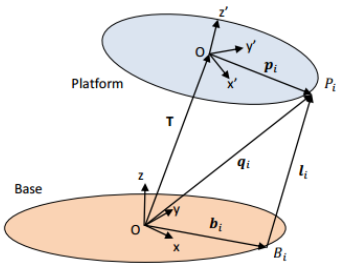

We choose the coordinate system originated at the center of the exoskeleton's bottom ring to be our default coordinate (base) system—**B**, and the attachment point between each actuator and the bottom ring[9] can be found using Creo's measurement tool and expressed as

$$B_i^B = \begin{bmatrix} X_i^B \\ Y_i^B \\ Z_i^B \end{bmatrix}, i = 1, 2, 3, 4, 5, 6.$$

We then define the coordinate system originated at the center of the top ring to be the local coordinate system **A**, so that the attachment point between the actuator and the bottom ring can be expressed as

[9] The end of the actuator was fixated to a bracket-universal joint linkage which was then mounted onto the bottom ring. We took account for the extra length in the y-coordinate system in our actual calculation.

$$A_i^A = \begin{bmatrix} x_i^A \\ y_i^A \\ z_i^A \end{bmatrix}.$$

A translation matrix $\boldsymbol{T} = \begin{bmatrix} x \\ y \\ z \end{bmatrix}$ is required to transfer points between the two coordinate systems. Since the bottom and top rings are designed to be co-axial when held parallel and we would constrain our SP to perform only pitch and yaw rotations (about X and Z axes), the translation along the Y-axis should remain constant during full range of motions. [10]

The top ring's rotation about X and Z axes would lead to two rotational matrices $\boldsymbol{Rt_X}$ and $\boldsymbol{Rt_z}$[11]. We define angular displacements about the two axes to be θ and α, respectively. The total rotational matrix is the product of $\boldsymbol{Rt_X}$ and $\boldsymbol{Rt_z}$:

$$\boldsymbol{Rt} = \boldsymbol{Rt_X} * \boldsymbol{Rt_z} = \begin{vmatrix} 1 & 0 & 0 \\ 0 & cos\theta & sin\theta \\ 0 & -sin\theta & cos\theta \end{vmatrix} * \begin{vmatrix} cos\alpha & sin\alpha & 0 \\ -sin\alpha & cos\theta & 0 \\ 0 & 0 & 1 \end{vmatrix}$$

Thus, expressing any point on the top ring in the base ring coordinate system at any configuration can be achieved by the following equation:

$$A_i^B = \boldsymbol{T} + A_i^A * \boldsymbol{Rt}$$

Where A_i^B means point A on the top ring expressed in the base ring coordinate system B. Finding the length between these two points can be easily achieved by conducting a vector length calculation. So eventually, the length of each actuator can be calculated as

$$l = \left| A_i^B - B_i^B \right|$$

Creo's measurement tool measures the coordinates of each top ring attachment point using the default coordinate system (in our case, the coordinate system originated at the center of the bottom ring), which can serve as a verification to our own calculation. Our calculation matches up closely with the Creo's result.

In contrast to inverse kinematics of a SP, which has a finite solution, the forward kinematics of a SP has no general form of solution and can be only approximated by optimization (Jakobivic and Budin). Additionally, inverse kinematics would be able to sufficiently serve the purpose of controlling our wrist exoskeleton since we would know the desired configuration and the only required variables to be found are the corresponding length of each actuator.

Specifications and Parameter Analysis: Creo's Position Analysis

As specified in the Inverse Kinematic Analysis discussion, the forward kinematics for a SP cannot be easily solved in a general form. As a result, our control of the SP for the exoskeleton relies heavily on the positional accuracy of the inverse kinematics. The position function in Creo provided the necessary information to compare our MATLAB script's output to what we witness in our Creo assembly. In the figures below, the plot of actuator length versus input angle—θ and α—show the relationship between the desired configuration and the necessary link lengths for all 6 linear actuators. These results conclude that we are able to determine the necessary lengths of each

[10] Jakobovic, Domagoj, and Leo Budin. "Forward Kinematics of a Stewart Platform Mechanism." (2002): n. pag. Print.

[11] We would like to explore the roll motion at wrist which is actually executed by the elbow joint if time allows. The roll motion will require an additional matrix to take account of rotation about Y-axis.

actuator to produce the desired output given the pitch and yaw rotational inputs of the SP.

There is some source of error in the values calculated by the MATLAB script and the measurement values obtained from Creo, but because they fall within a 3% margin of error, this error was taken to be negligible.

MATLAB graphical representation of position analysis

As shown in the *Figure 1*, our MATLAB code predicts the position of each actuator in our SP. As expected from our initial analysis by hand, the position analysis reveals that here are 3 sets of 2 actuators with equivalent length at all points during rotation about the x-axis. To be exact the red color is represented by both L_1 and L_2. Black represents actuators L_3 and L_6. Blue represents actuators L_4 and L_5. By geometrical symmetry simplification provided through the predefined attachment points of the actuators, this prediction can be supported.

Figure 1: X-Axis Rotation

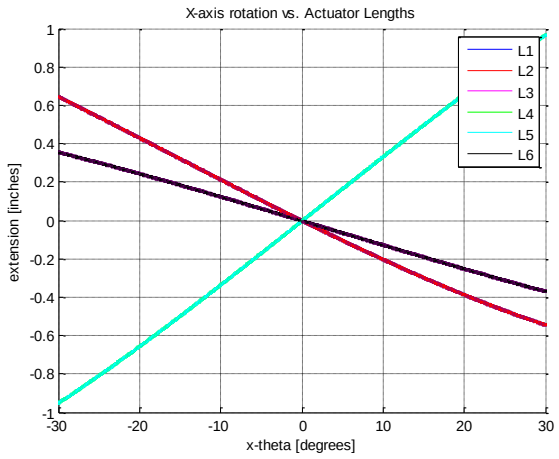

In addition, when taking into account the symmetrical structure about the z-axis, we also predicted (due to the symmetrical structure) that pure rotation about the z-axis should result in 2 sets of 3 actuators with equivalent length for all points. This prediction was affirmed with our MATLAB simulation shown in *Figure 2*. Each color represents 3 actuators of each length and symbolically represents the movement of the SP from -30 to 30 degree rotation about the z-axis. This is the equivalent of moving the full range within the radial and ulnar[12] directions of the wrist motion, according to the Department of Social & Health Services. Blue represents the actuator lengths of L_1, L_3, and L_5. Black represents the actuator lengths of L_2, L_4, and L_6.[13]

Figure 2: Z-axis Rotation

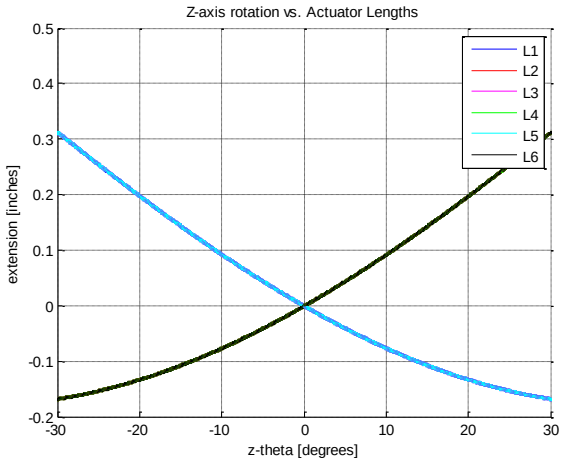

Figure 3 demonstrates the predictions made in MATLAB to simulate the wrist rotation at a 10 degree tilt. This simulation is the equivalence of forming a fist in extension at 10 degrees and rotating the fist in a conical shape. The well defined behavior demonstrates that our

[12] Department of Social & Health Services

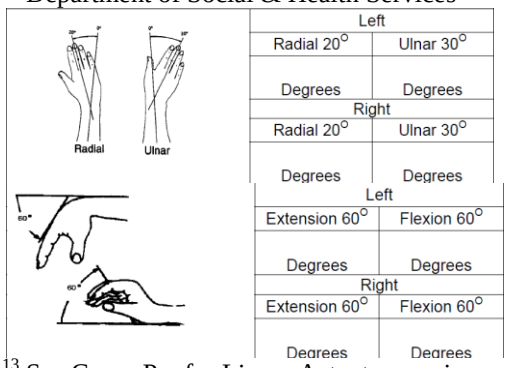

[13] See Cover Pg. for Linear Actuator naming convention

SP is capable of achieving the necessary workspace to mimic the human wrist motion.

Figure 3: 10 Degree tilt vs. Actuator Length variation

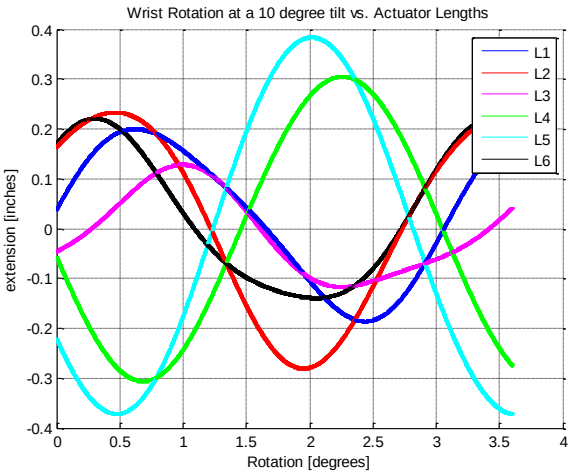

According to the specifications sheets provided by Firgelli Technologies, the stroke length for each L12 Actuator is 50mm with an accuracy of 0.2mm. Converting to inches, we see that our stroke length is 1.9685 inches. Therefore, by constraining the initial state of the SP to about the middle length settings, we allow for about 1 inch extension and contraction (0.98425inches to be exact). The maximum extension and contraction of the linear actuators places another constraint on the workspace of our SP. However, by analyzing the MATLAB plots, it is concluded that these rotational conditions can theoretically be repeated in our prototype because the extent of elongation and contraction of the actuator falls within the +/- 1inch.

To further highlight the usefulness of the MATLAB numerical analysis of the position of the SP, a similar function was selected as the input for the z and x axis of Creo to create this sinusoidal conical workspace of the human wrist. A simple out-of-phase constraint for the 2 rotating axis in Creo allowed us to recreate the motion described in *Figure 3* in a visual capacity; thereby confirming the capabilities of the SP with regards to achieving the desired workspace.

Creo graphical representation of position analysis

To confirm the analysis completed by our MATLAB numerical simulation, we performed a positional analysis through Creo. For simplicity, the analysis was only conducted along the x-axis for the SP in Creo. However, given an accurate prediction in the rotation about z-axis when compared to the MATLAB simulation will confirm an accurate prediction for each case explored in the previous section.

Figure 4: Creo's X-axis Rotation

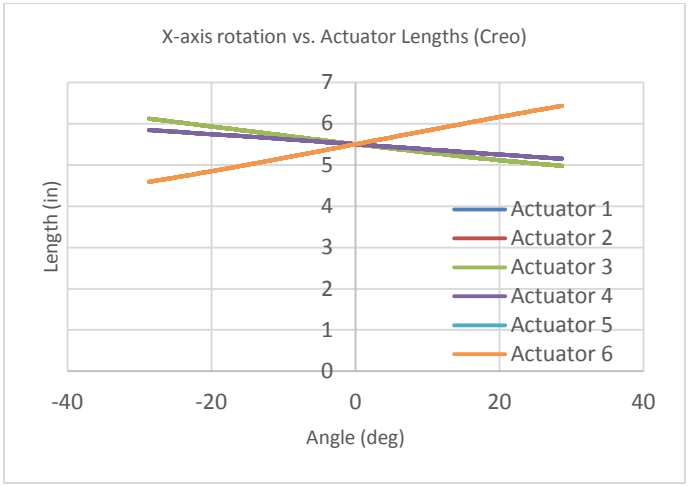

Although it may not be apparent at first glance, the predictions shown in Creo agree with the predictions made from MATLAB. *Figure 4* demonstrates the data collected from Creo's measurement analysis and is shown in absolute value of the actuator lengths whereas MATLAB is shown in relative motion of the actuator. Therefore, by taking the values of each point along the x-axis rotation and subtracting the initial value of the actuator lengths when the SP is at its starting point reveals a direct comparison to *Figure 1*. Thus, the positional analysis conducted by Creo and MATLAB, two powerful engineering tools, agree with one another within

a 3% margin. As a result, the inverse kinematics produces desirable conclusions for our SP.

Figure 5: Creo's X-axis Rotation (Relative Stroke Length)

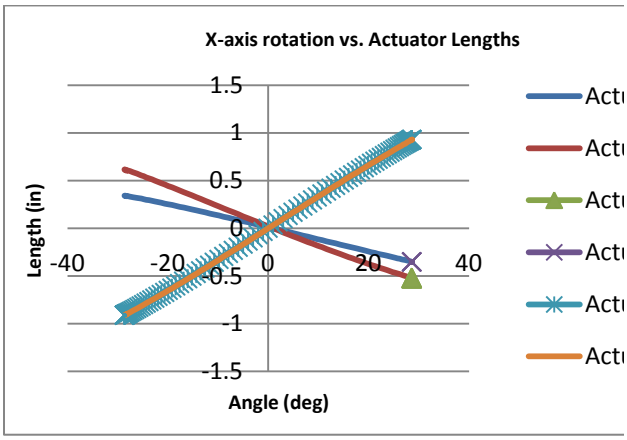

Specifications and Parameter Analysis: Force Analysis

In order to determine the force necessary from each actuator given a load, force analyses were conducted in Creo. It is crucial to confirm that each actuator does not experience a load that is greater than its allowable threshold[14]. Each analysis was conducted with four individual loads of 2.5 lbs, each force facing down on the ends of the upper ring[15]. The total force adds up to 10 lbs, the heaviest load expected on the design. There were three analyses conducted for three different positions: one at original orientation (θ=0°), one at roughly maximum pitch (θ=27°), and one at roughly maximum yaw (θ=17.5°). The results are as follows:

Table 1: Resulting Force (lbs) at Varying Orientations

Actuator	θ = 0°	θ_{pitch} = 27°	θ_{yaw} = 17.5°
1	-1.10225	-4.67789	-4.78545
2	-0.698163	1.58797	0.78458
3	0.511952	-2.02981	2.72771
4	**0.511952**	**-1.66335**	**-6.21019**
5	-0.698163	1.75242	-2.80175
6	-1.10225	-4.93368	0.462132

The bolded text indicates the highest force experienced by the linear actuators. The highest force falls within the factor of safety specified in the technical sheets attached in the appendix from Firgelli.

Figure 6a: Front View of Original Orientation

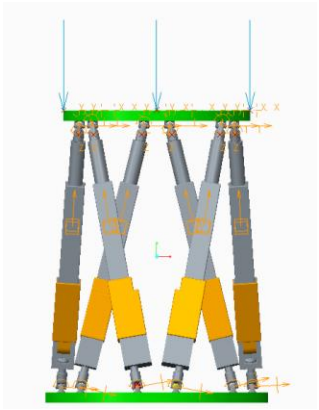

Figure 6b: Right View of Original Orientation

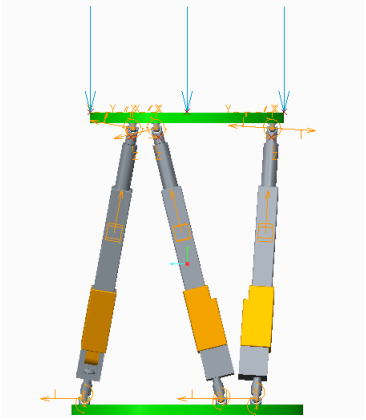

[14] The actuators can experience 45 N (10.116 lbs) of force before backdrivability.
[15] Coordinates: (0, 7.03425, 2.25), (0, 7.03425, -2.25), (2.25, 7.03425, 0), (-2.25, 7.03425, 0)

Figure 7: Front View of Maximum Pitch

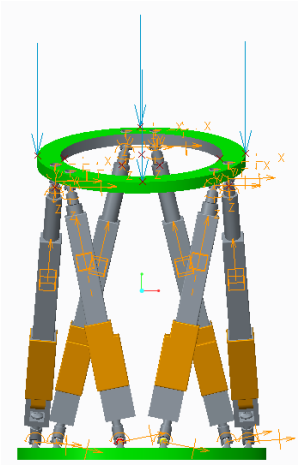

Figure 8: Right View of Maximum Yaw

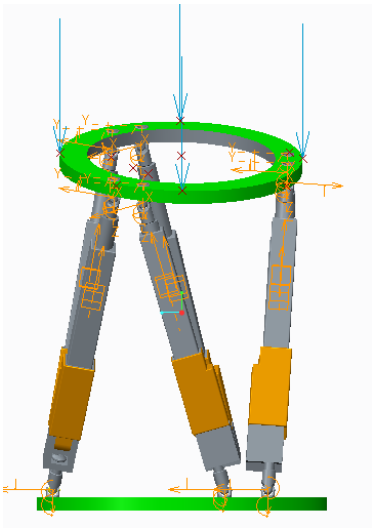

To verify Creo's force analyses, a force analysis was conducted by hand at the original orientation. There are 6 unknowns so 6 equations are necessary. The sum of forces along the x-, y-, and z-axes are given below:

$$\sum F_x = A_x \cos\alpha_1 - B_x \cos\alpha_2 + C_x \cos\alpha_3 - D_x \cos\alpha_3 + E_x \cos\alpha_2 - F_x \cos\alpha_1 = 0$$

$$\sum F_y = A_y \cos\beta_1 + B_y \cos\beta_2 + C_y \cos\beta_3 + D_y \cos\beta_3 + E_y \cos\beta_2 + F_y \cos\beta_1 - L = 0$$

$$\sum F_z = A_z \cos\gamma_1 - B_z \cos\gamma_2 - C_z \cos\gamma_3 - D_z \cos\gamma_3 - E_z \cos\gamma_2 + F_z \cos\gamma_1 = 0$$

The sum of moments about point O is:

$$\sum M_O = r_A \times A + r_B \times B + r_C \times C + r_D \times D + r_E \times E + r_F \times F + r_L \times L = 0$$

where L is the applied load.

The final three equations are given by the sum of moments about the x-, y-, and z-axes at point O:

$$\sum M_{O,x} = (r_A \times A)\cdot\bar{\imath} + (r_B \times B)\cdot\bar{\imath} + (r_C \times C)\cdot\bar{\imath} + (r_D \times D)\cdot\bar{\imath} + (r_E \times E)\cdot\bar{\imath} + (r_F \times F)\cdot\bar{\imath} + (r_L \times L)\cdot\bar{\imath} = 0$$

$$\sum M_{O,y} = (r_A \times A)\cdot\bar{\jmath} + (r_B \times B)\cdot\bar{\jmath} + (r_C \times C)\cdot\bar{\jmath} + (r_D \times D)\cdot\bar{\jmath} + (r_E \times E)\cdot\bar{\jmath} + (r_F \times F)\cdot\bar{\jmath} + (r_L \times L)\cdot\bar{\jmath} = 0$$

$$\sum M_{O,z} = (r_A \times A)\cdot\bar{k} + (r_B \times B)\cdot\bar{k} + (r_C \times C)\cdot\bar{\bar{k}} + (r_D \times D)\cdot\bar{k} + (r_E \times E)\cdot\bar{k} + (r_F \times F)\cdot\bar{k} + (r_L \times L)\cdot\bar{k} = 0$$

Specifications and Parameter Analysis: Dimensional Description

The nature of our exoskeleton requires us to proceed to our design closely following human forearm/wrist parameters. We determined the wrist diameter, forearm length, forearm diameter, and so forth by taking the average measurement of each group member's forearm. Since the product is intended to serve patients with physically impaired wrists, we designed our device to be easily wearable by enlarging the diameters of the SP rings (top and bottom). We also took account of the difference between people's forearm length by implementing a length adjustment mechanism at the bottom of our exoskeleton.

The rest of our design's dimensions were determined by the size of the linear actuators we chose. The most appropriate actuators were 5.5" when held at the SP's resting position, which dictated the total length of our exoskeleton to be around that length. After finding proper sized universal joints and assembling the two rings, we set the total length of the SP to be 7''. Velcro strips can be applied as means to attach our device to human arm so some of the parameters can be adjustable.

Design Risks:

The main risk in the exoskeleton is that there is no mechanical stop. Our design is purely driven by an implemented control system. While the maximum range of motion of the design does not exceed the average range of the human wrist, the lack of mechanical stop is still a concern. The difficulty in applying the control system is an additional risk; if the control system is not appropriately created, the exoskeleton will not function properly.

The circular components of the exoskeleton bring forth some manufacturing and some assembly concerns, which are further complicated by the limited workspace of the wrist.

Manufacturing Processes:

The following chart briefly describes the manufacturing processes required to craft each individual part in the SP. In addition, the purchases and already obtained materials are noted. Given the complexity of some of the parts, we simplified all milling operations and use of the lathe required to a categorical specification rather than explicitly defining the machining procedure.

Table 2: Manufacturing/Product Summary

Company	Product	Product no.	Price	Qty
Firgelli	L12 Linear Actuator	L12-50-210-12-I	$90	6
SDP	0.75 " Acetal U-joint	A 5T 8-D206	$3.88	12
BeagleBoard	BeagleBone Black		$45	1
Machined	Top Disk	CNC-Mill		
	Bottom Disk	CNC-Mill		
	Joint top	CNC-Mill		
	Joint bottom	CNC-Mill		
	Joint attachment	CNC-Mill		
	Grip	Lathe		
	Grip Bar	Pressed Metal		
	Attachment Cylinder	Band/Hacksaw		
Acquired	Velcro			
	Screws			
	Batteries			

According to our predictions made in *Table 2* we expect to purchase $631.56 (excluding tax & shipping) on this Senior Design project. We also expect to be machining 6 parts for the exoskeleton and SP design. Due to the structure sturdiness that is required of

exoskeleton, the 3D printer will not be considered as a possible substitute to machining products.

Material selection:

We have decided to use either Delrin or aluminum to machine the SP rings. Both of the materials would be strong enough to withstand the load/moment incurred during its movement but aluminum would probably undergo less deformation during machining process. The brackets connecting linear actuators to the universal joints will be machined out of aluminum to achieve desired level of strength; the length adjustment piece and elbow joint will also be machined out of aluminum. The connecting part between the SP and the elbow joint will be made out of a large PVC pipe. The elastic band securing patient's hand will be connected to the SP by an aluminum frame. Elastic material like foam and stretchable fabrics will be applied to surface/point on the exoskeleton where it contacts with human forearm.

Microcontroller and Actuator Selection:

Due to the large workspace, biomechanical subject, and the kinematic procedures, a microcontroller board with a large onboard memory and fast processing speeds was determined to be appropriate for this project. The BeagleBone Black supplies both of these. To simplify the circuitry and connections, the linear actuators were selected with integrated control boards for position control via RC, PWM, or servo inputs. Furthermore, to supply the required force of 45N, a gearbox of gear ratio 210:1 was selected.

Conclusion:

Although the Stewart Platform (SP) presented a number of difficulties in performing the forward kinematics of the mechanism, the accessible results from the inverse kinematics greatly aided our design efforts. Through the powerful engineering tools of MATLAB and Creo, we have supported the mathematical foundation of the SP's mechanism behavior as a function of input angles. Thus, by having the positional analysis and the force analysis completed on our SP design, we have concluded that our design falls within the required strength and kinematic requirements to sustain the application of our SP—that is to provide rehabilitation through mobility-gait training with an assistive device.

APPENDIX

MATLAB CODE: Inverse Kinematics for actuator lengths

setup.m

```
h = 6.75;
b1 = [-.46462; 0.375; 2.39026];
b2 = [0.46462; 0.375; 2.39026];
b3 = [2.30234; 0.375; -.792758];
b4 = [1.83772; 0.375; -1.5975];
b5 = [-1.83772;0.375; -1.5975];
b6 = [-2.30234;0.375; -.792758];
t1 = [-1.55429; 6.625; 1.25864];
t2 = [1.55429; 6.625; 1.25864];
t3 = [1.86716; 6.625; 0.716736];
t4 = [.312896; 6.625; -1.97538];
t5 = [-.312869; 6.625; -1.97538];
t6 = [-1.86716; 6.625; 0.716736];
xtheta=0;
ytheta=0;
ztheta=0;
```

SP.m

```
function [ L1,L2,L3,L4,L5,L6 ] =
SP(
h,b1,b2,b3,b4,b5,b6,t1,t2,t3,t4,t5,
t6,xtheta,ytheta,ztheta )

H=[0;h;0];
xrad=xtheta*pi/180;
yrad=ytheta*pi/180;
zrad=ztheta*pi/180;

R=rotx(xrad)*rotz(zrad)*roty(yrad);
t1n=R*(t1-H)+H;
t2n=R*(t2-H)+H;
t3n=R*(t3-H)+H;
t4n=R*(t4-H)+H;
t5n=R*(t5-H)+H;
t6n=R*(t6-H)+H;

L1=pdist2(b1',t1n')
L2=pdist2(b2',t2n')
L3=pdist2(b3',t3n')
L4=pdist2(b4',t4n')
L5=pdist2(b5',t5n')
L6=pdist2(b6',t6n')

end
```

testrotations.m

```
hold on
for xdiff=-30:.1:30
    xtheta=xdiff;
    ytheta=0;
    [ L1,L2,L3,L4,L5,L6 ]=SP(
h,b1,b2,b3,b4,b5,b6,t1,t2,t3,t4,t5,
t6,xtheta,ytheta,ztheta );
    plot(xdiff,L1,'+');
    plot(xdiff,L2,'r');
    plot(xdiff,L3,'y');
    plot(xdiff,L4,'g');
    plot(xdiff,L5,'c');
    plot(xdiff,L6,'k');
end

figure
hold on
for ydiff=-30:.1:30
    ytheta=ydiff;
    xtheta=0;
    [ L1,L2,L3,L4,L5,L6 ]=SP(
h,b1,b2,b3,b4,b5,b6,t1,t2,t3,t4,t5,
t6,xtheta,ytheta,ztheta );
    plot(ydiff,L1,'+');
    plot(ydiff,L2,'r');
    plot(ydiff,L3,'y');
    plot(ydiff,L4,'g');
    plot(ydiff,L5,'c');
    plot(ydiff,L6,'k');
end
```

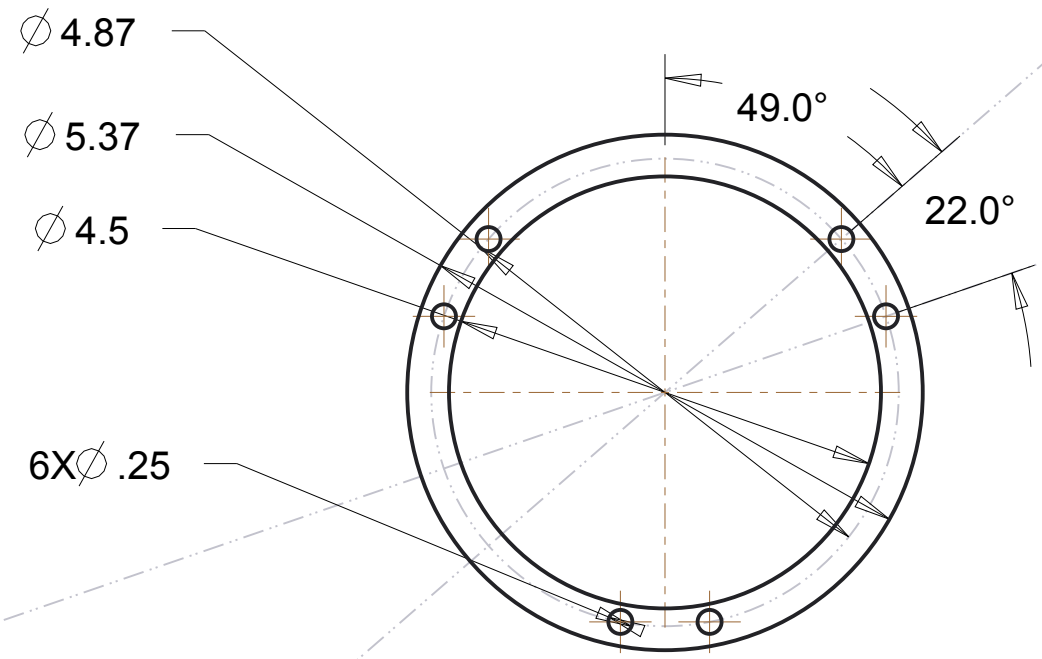

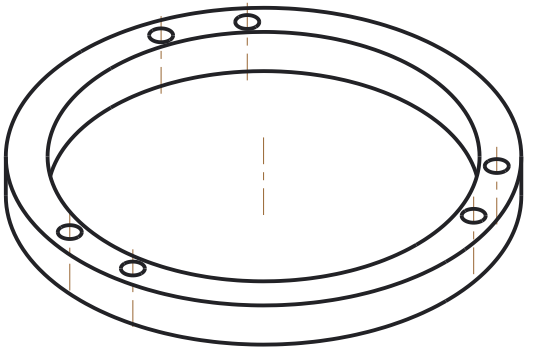

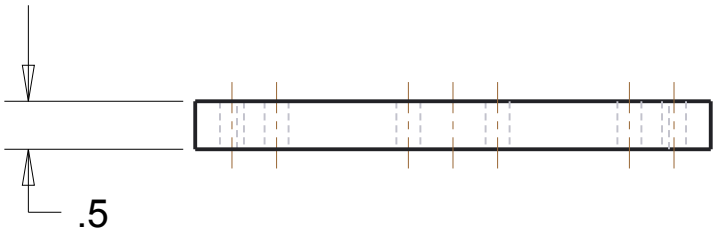

IDX NO:1	SP_Bottom_Ring	QTY:1	DWG NO:1

PARTS LIST

Senior Design

TITLE

ILT Exoskeleton

SIZE	MATERIAL	DWG NO	REV
A	Aluminum	###-##	0

DWN	ILT	02/10/14	SCALE: 1/2	INCHES	SHEET # OF #

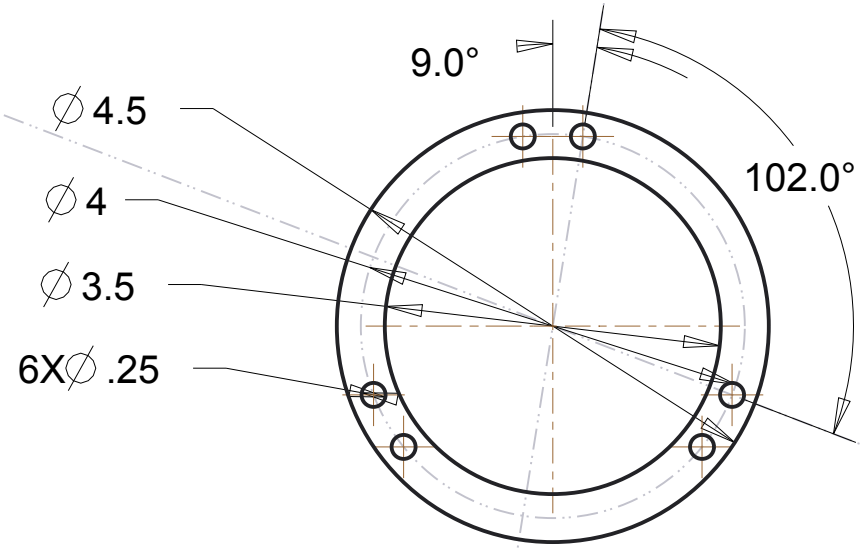

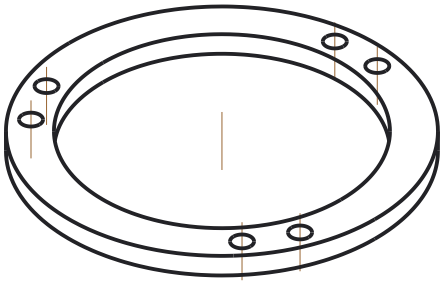

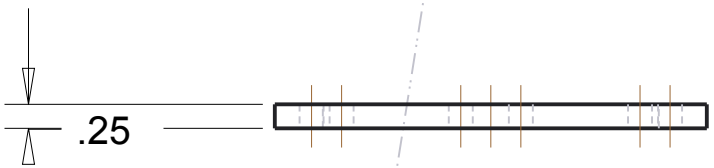

IDX NO:2	SP_Upper_Ring	QTY:1	DWG NO:2

PARTS LIST

Senior Design

TITLE

ILT Exoskeleton

SIZE	MATERIAL	DWG NO	REV
A	Aluminum	###-##	0

DWN	ILT	02/10/14	SCALE: 1/2	INCHES	SHEET # OF #

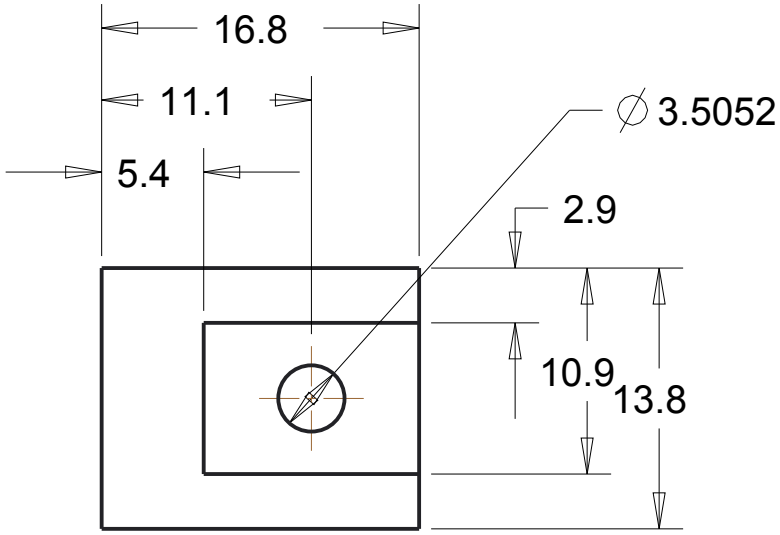

SCALE 2.500

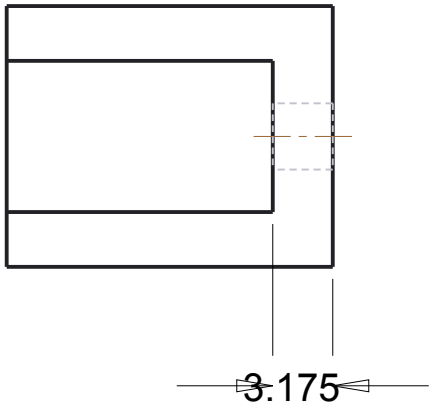

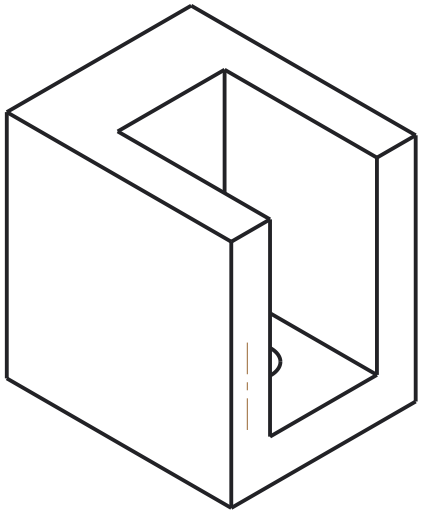

SCALE 2.500

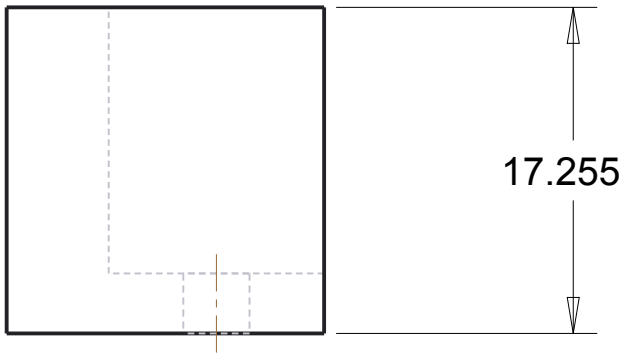

IDX NO:3	SP_Mounting_Bracket	QTY:6	DWG NO:3

PARTS LIST

Senior Design

TITLE

ILT Exoskeleton

SIZE	MATERIAL	DWG NO	REV
A	Aluminum	###-##	0

DWN	ILT	02/10/14	SCALE: 1/2.5	MILLIMETERS	SHEET # OF #

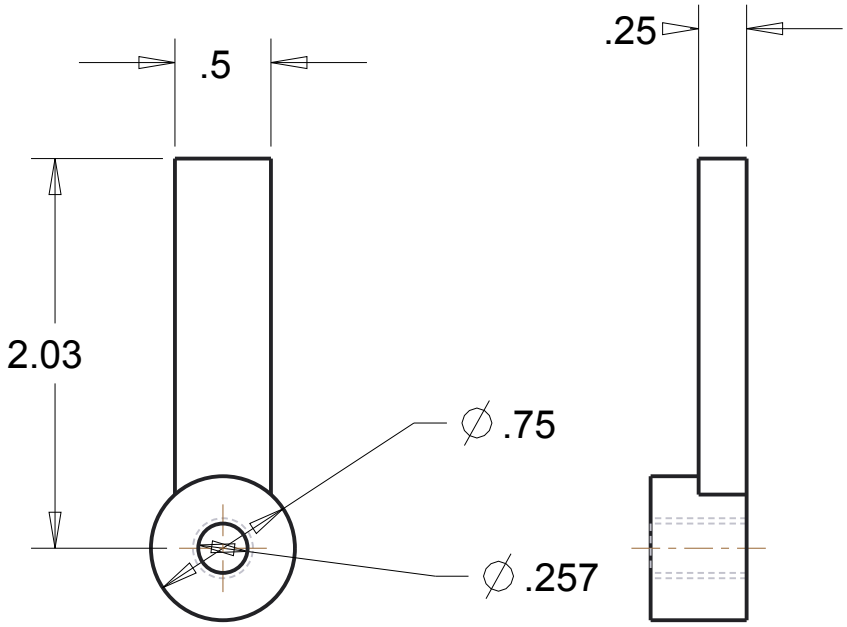

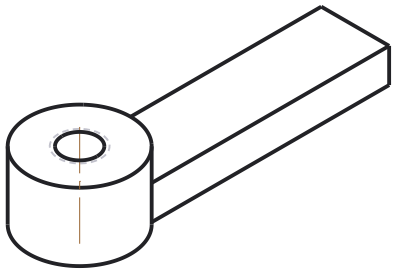

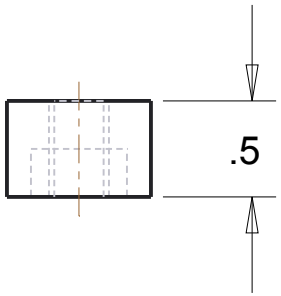

IDX NO: 4	Elbow_Joint_Inner_Part	QTY:1	DWG NO:4

PARTS LIST

Senior Design

TITLE

ILT Exoskeleton

SIZE	MATERIAL	DWG NO	REV
A	Aluminum	###-##	0

DWN	ILT	02/10/14	SCALE: 1/1	INCHES	SHEET # OF #

SECTION XSEC0001-XSEC0001

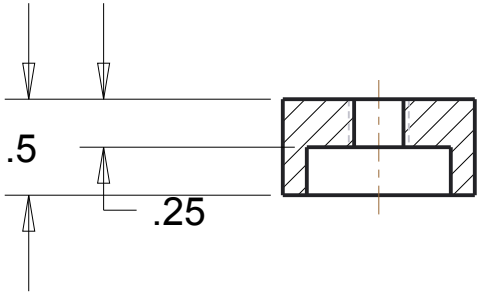

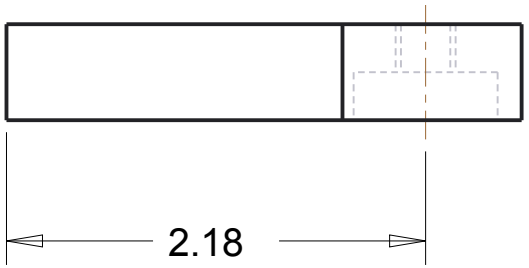

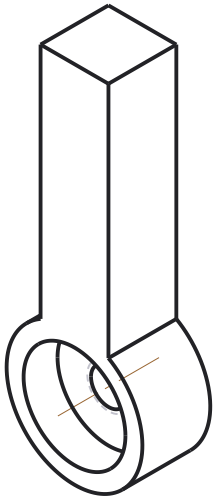

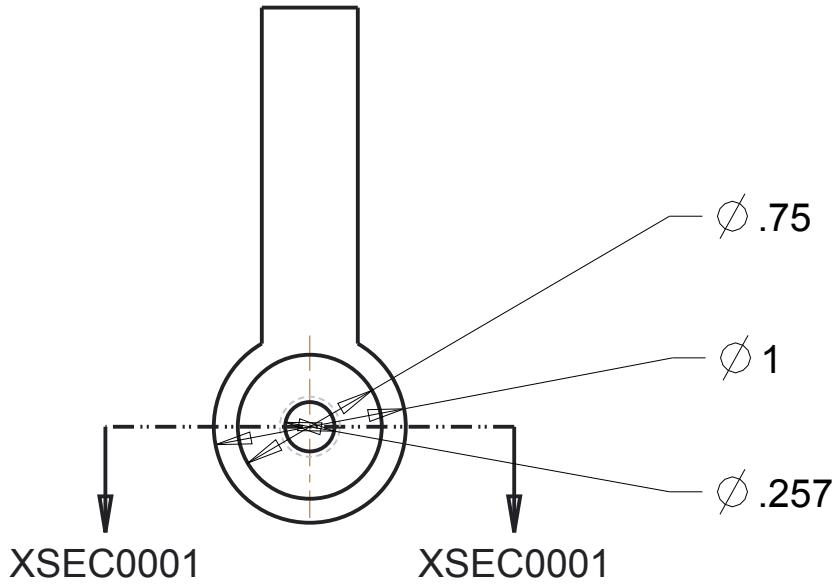

IDX NO:5	Elbow_Joint_Outer_Part	QTY:1	DWG NO:5
PARTS LIST			

Senior Design

TITLE

ILT Exoskeleton

SIZE	MATERIAL	DWG NO	REV
A	Aluminum	###-##	0

DWN	ILT	02/10/14	SCALE: 1/1	INCHES	SHEET # OF #

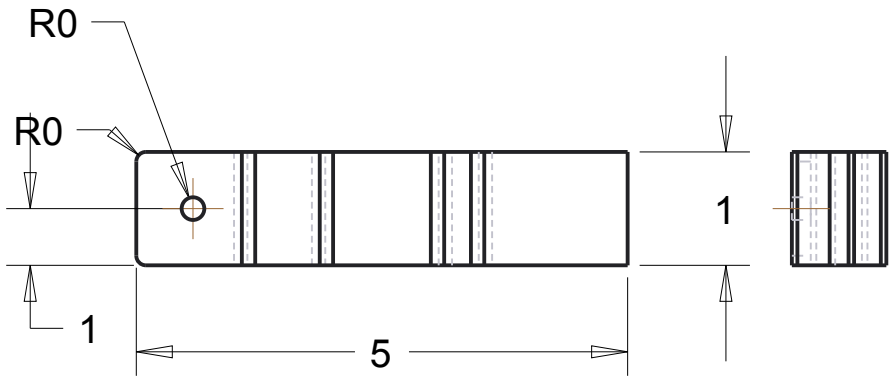

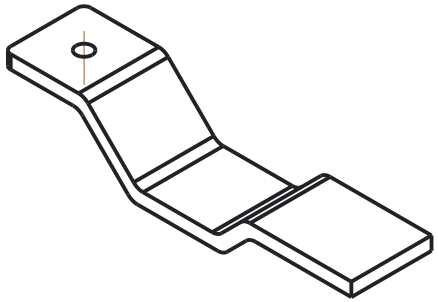

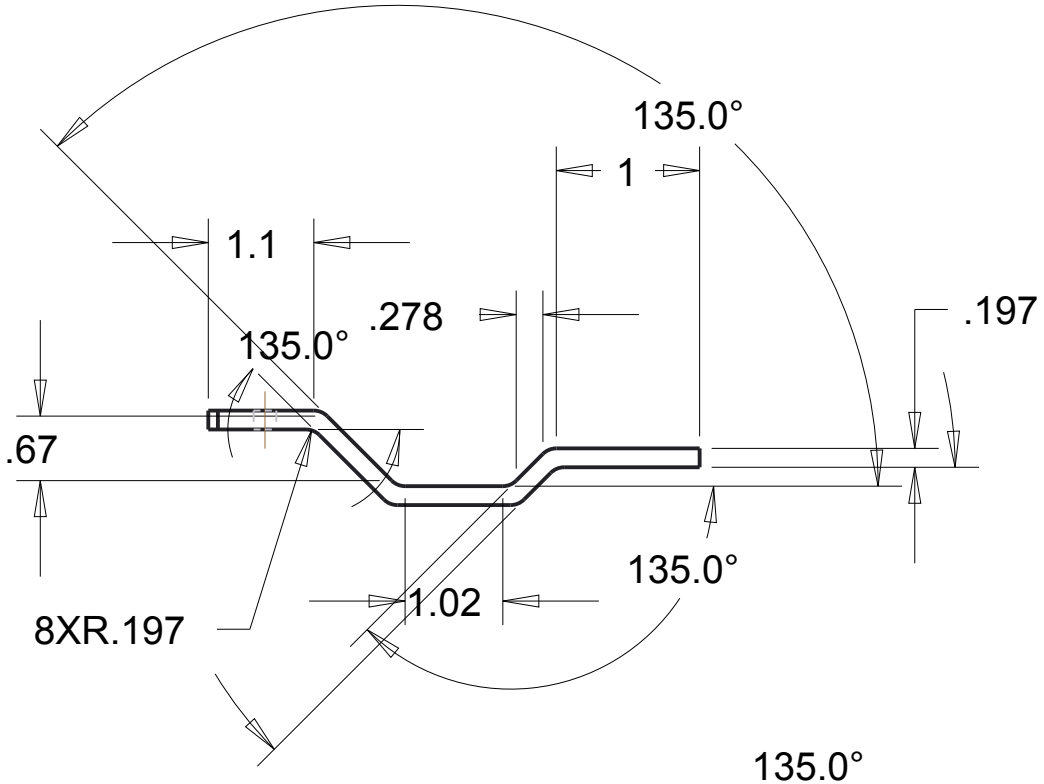

IDX NO:6	Hnad_Grip_Frame	QTY:1	DWG NO:1

PARTS LIST

Senior Design

TITLE

ILT Exoskeleton

SIZE	MATERIAL	DWG NO	REV
A	Aluminum	###-##	0

DWN	ILT	02/10/14	SCALE: 1/2	INCHES	SHEET # OF #

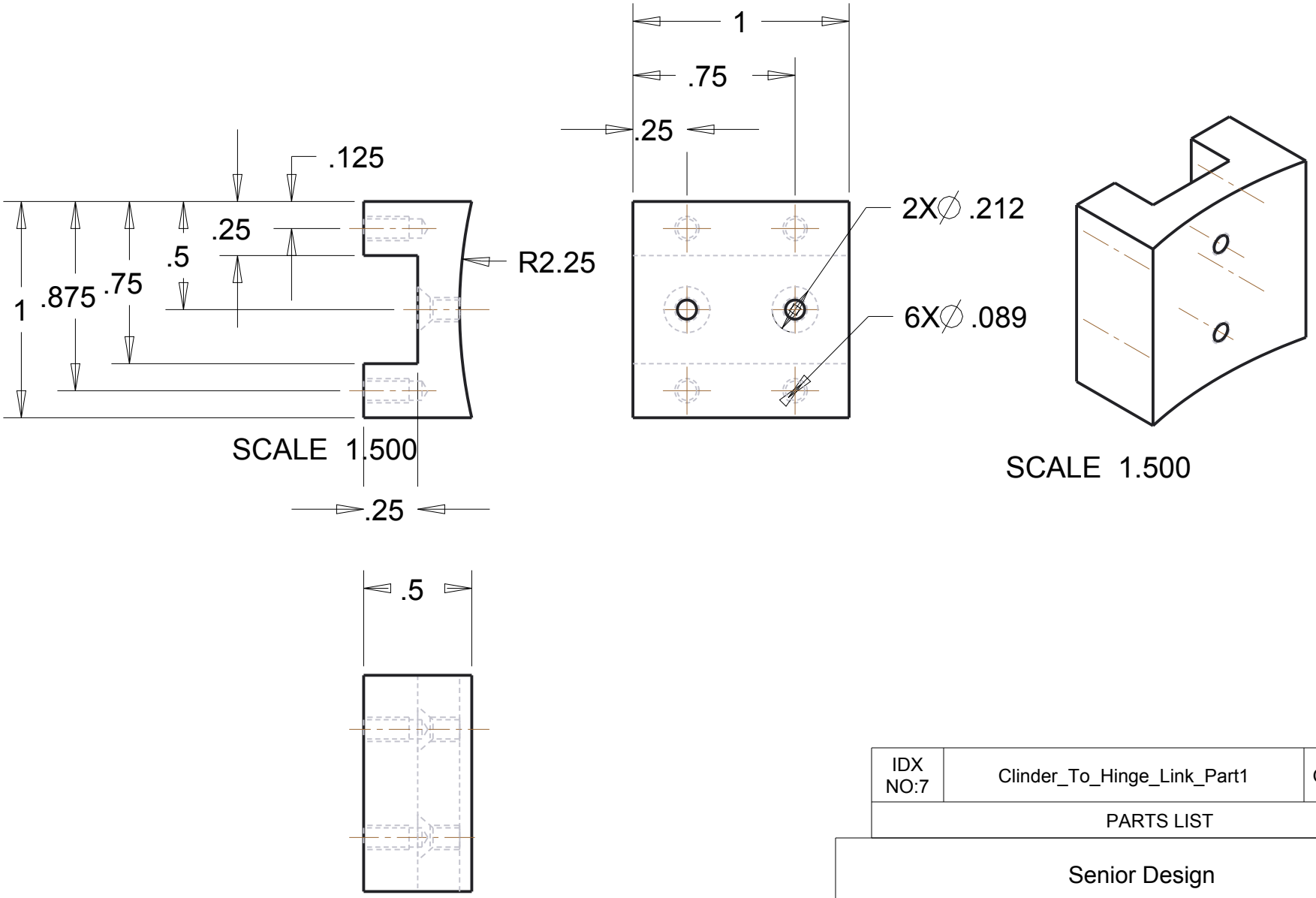

IDX NO:7	Clinder_To_Hinge_Link_Part1	QTY:1	DWG NO:7

PARTS LIST

Senior Design

TITLE

ILT Exoskeleton

SIZE	MATERIAL	DWG NO	REV
A	Aluminum	###-##	0

DWN	ILT	02/10/14	SCALE: 1/1.5	INCHES	SHEET # OF #

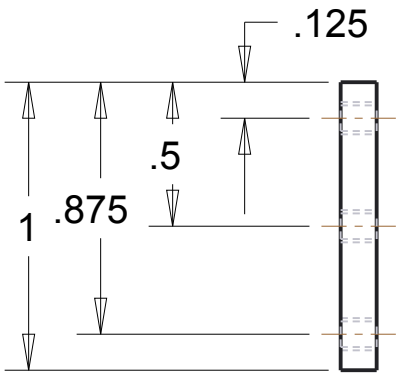

SCALE 1.500

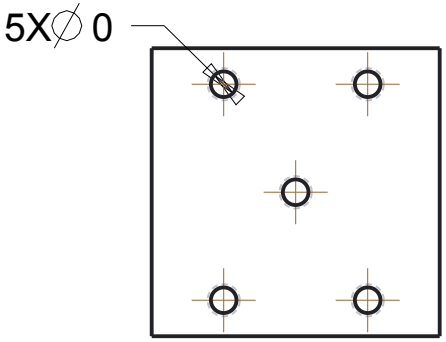

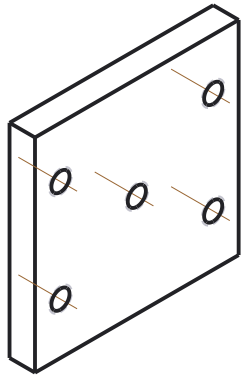

SCALE 1.500

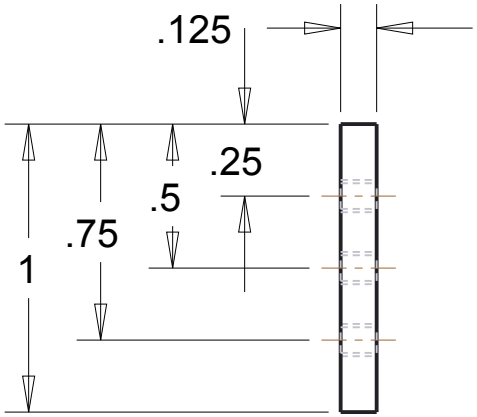

IDX NO:8	Cylinder_To_Hinge_Link_Part2	QTY:1	DWG NO:8

PARTS LIST

Senior Design

TITLE

ILT Exoskeleton

SIZE	MATERIAL	DWG NO	REV
A	Aluminum	###-##	0

DWN	ILT	02/10/14	SCALE: 1.5/1	INCHES	SHEET # OF #

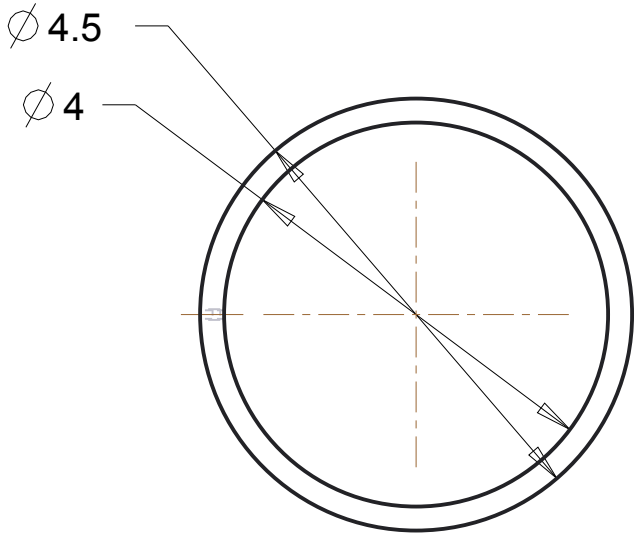

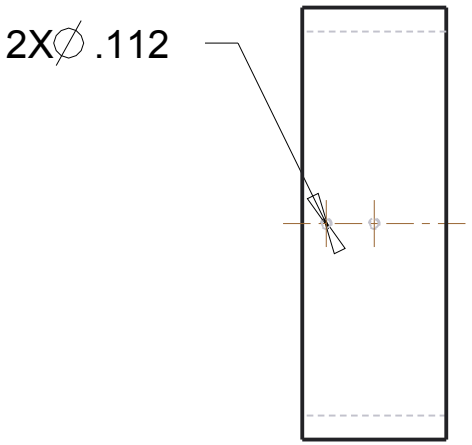

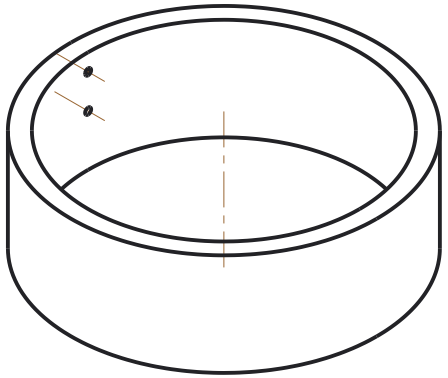

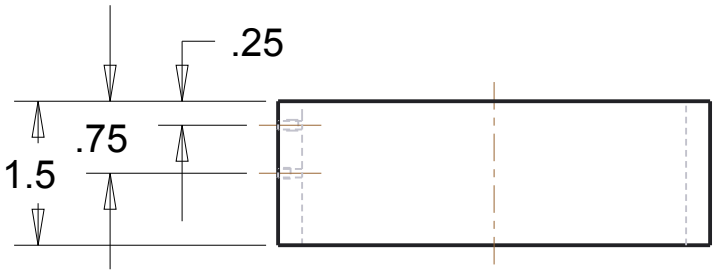

IDX NO:9	Cylinder_Conncecting_To SP_Bottom	QTY:1	DWG NO:9

PARTS LIST

Senior Design

TITLE

ILT Exoskeleton

SIZE	MATERIAL	DWG NO	REV
A	PVC Pipe	###-##	0

DWN	ILT	02/10/14	SCALE: 1/2	INCHES	SHEET # OF #

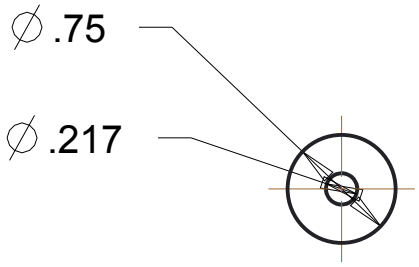

SCALE 0.750

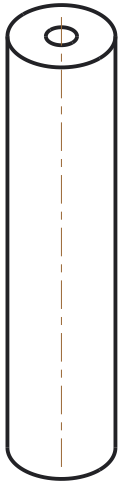

SCALE 0.750

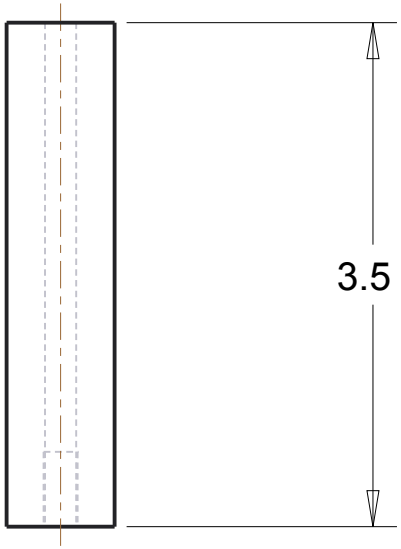

IDX NO:10	Hand_Grip_Bar	QTY:1	DWG NO:10

PARTS LIST

Senior Design

TITLE

ILT Exoskeleton

SIZE	MATERIAL	DWG NO	REV
A	Delrin	###-##	0

DWN	ILT	02/10/14	SCALE: 3/4	INCHES	SHEET # OF #